PERFORMANCE CHARACTERISTICS AND PERMITTIVITY MODELLING OF A SURFACE PLASMON RESONANCE SENSOR FOR NON DESTRUCTIVE METAL SURFACE MONITORING IN A SALINE MARITIME ENVIRONMENT

Dr CR Lavers University of Lincoln UK Clavers@Lincoln.ac.uk Dr AM Cree, Dr D Jenkins, Mr N Salah, and Mr M Findlay
Plymouth University UK

2nd LOGO

UNIVERSITY OF LINCOLN

INTRODUCTION

We evaluate the suitability of Surface Plasmon Resonance (SPR), an established optical sensing mode, to quantify surface parameters (real & imaginary permittivity, and thickness) for relatively inert thin silver films exposed to a synthetic marine standard solution. Metal layers exhibit long-term durability, yet exhibit detectable linear temporal reflectivity changes at the surface recorded in SPR minimum angle curves. Sensor design was achieved with Fresnel's optical theory for isotropic multi-layer media. We developed a data-fitting routine, yielding numerical permittivity and thickness solutions for 'corroded ' surfaces.

Many attempts have been made to create accurate surface monitoring corrosion sensors, which suffer from inability to detect corrosion at low levels before serious damage is done. Corrosion may occur in inaccessible undersea pipelines or enclosed areas; it is hard to predict where or when this will occur. Corrosion-related fracture detection with optical sensors *may* reduce fleet or offshore structure maintenance costs. Sensors for optical applications include optical fibres [**1**] or ellipsometry [**2**] where thickness and refractive index, must be known, whilst SPR can determine both. SPR sensors provide vital surface optical parameters (real and imaginary permittivity and thickness), or early corrosion change when corroded material removal may avoid costly structural repairs. SPR was used for aqueous sensing [**3**], with potential for corrosion-related detection. We present our SPR method for potential corrosion detection [**4**], evaluating the surface analytical technique to detect time-dependent thin film corrosion, and from data-fitting provide quantified permittivity values.

Corrosion and mechanical damage are key failure modes

Apart from lost lives or disasters, it is estimated the global annual corrosion in on / off shore metal pipelines exceeds $2.5 trillion [**5**]. In the USA 1998-2017, 306 fatalities and 1259 injuries were related to oil, gas or hazardous fluid pipeline failure, costing > $8.1 billion. Corrosion-induced failure is a key concern in maintaining pipeline integrity. Annually thousands of barrels of oil spill into seas from corroded pipes. Corrosion may go undetected until components fail, or are irreparably damaged, often catastrophically. In 1992 a Guadalajara petrochemical pipeline exploded killing 215 people, traced back to a corroded pipe.

Fracture is a recognised metal failure mode, often occurring without warning. Corrosion may induce ionic stress or strain surface concentrations. Work has studied metal corrosion effects, but less investigation of the optical properties in *thin* metal layers < 1 micron, prior to often rapid fracture. Fatigue and corrosion are key engineering issues with corrosion described as an oxidation reaction, pure metal removed and replaced by oxide layers which are often weaker and more brittle than pure metal, reducing performance, lifespan, even causing structural failure.

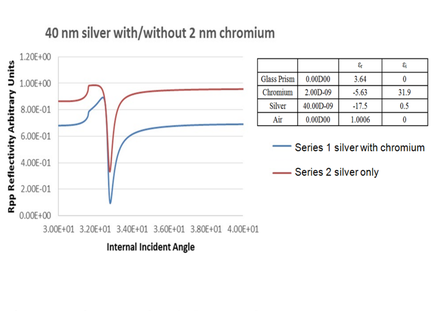

		ε_r	ε_i
Glass Prism	0.00D00	3.64	0
Chromium	2.00D-09	-5.63	31.9
Silver	40.00D-09	-17.5	0.5
Air	0.00D00	1.0006	0

Fig. 1 Theoretical SPR plot

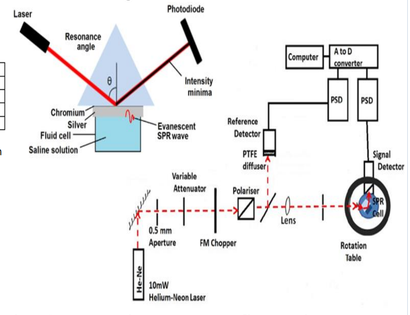

Fig. 2 Kretschmann configuration

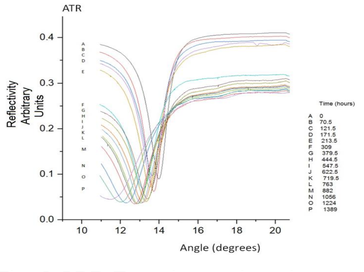

Fig. 3 SPR Experimental angle scans

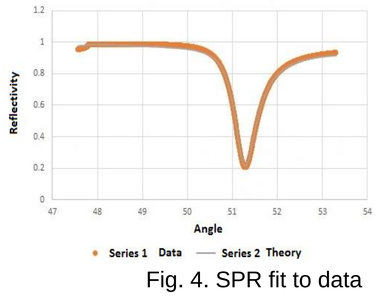

Fig. 4. SPR fit to data

THEORETICAL MODELLING

SPR Theory Transverse Magnetic (TM) light excites SPR at metal-dielectric interfaces. SPR are collective surface electron oscillations interacting with light. Both Otto [**6**] and Kretschmann [**7**] developed ways to achieve this, with the Kretschmann configuration used here and in previous work [**8-9**]. Surface corrosion includes changes to film thickness d, real / imaginary permittivity (εr and εi respectively); surface changes include change to εr and εi, or filling changes [**10**]. Mechanical properties are determined by local microstructure / texture under deposition or treatment, impacting corrosion susceptibility. Here thin coatings are deposited on thick substrates. SPR is supported between media with opposite sign of real parts of dielectric constant with exponentially decaying fields into each media, sensitive to changes in metal or dielectric :

$$\varepsilon_{,\,\text{real}} + \varepsilon_{,\,real} < 0 \quad (1)$$

When SPR is excited the wave-vector between 2 semi-infinite media is given by:

$$k_z = k_{SPP} = \frac{\omega}{c} \times \left(\frac{\varepsilon_{,\,\text{real}} \times \varepsilon_{,\,real}}{\varepsilon_{,\,\text{real}} + \varepsilon_{,\,real}} \right)^{0.5} = \sqrt{\varepsilon_{glass}} \times \frac{\omega}{c} \times \sin\theta \qquad (2)$$

(with z is along the interface, ω angular velocity, ε_{glass} dielectric constant, θ incident angle). The SPR wave-vector is highly sensitive to optical interfaces making it a valued technique for measuring film properties at boundaries supporting a resonance.

We modelled SPR coupling in FORTRAN by varying parameters, e.g. thickness, for optimisation. Our method calculates reflectivity as a function of incident angle for multi-layer media as a series of isotropic slabs of thickness less than a wavelength. A scattering method **[11]** accounts for reflection / transmission coefficients at interfaces between media, coupling incoming fields with a stable matrix. Scattering matrix output is shown for a 4-layer 652nm simulation with 2000 steps, **fig. 1.** Optical parameters are shown for a glass prism, chromium adhesion layer, silver, and air. SPR system modelling used film parameters taken from a recognised source **[12]**.

METHODS AND MATERIALS

SPR Experimental Arrangement

In the Kretschmann configuration we recorded reflectivity from synthetic saline samples over time **(fig. 2).** Chromium, and then silver were sputtered on glass. A He-Ne laser (632.8nm) provided coupling above the critical angle, stepped in angle under computer control. A FM chopper permitted signal and reference PSD with lock-in amplifiers to minimise noise. Data acquisition took place with a National Instruments USB 6210. A LabView program controlled a motorised rotation stage, recording diode reflectivities from sample / reference beams. A θ prism movement gave a 2θ diode turn, ensuring reflected beams strike the diodes. As the stage rotates we record reflected intensity against data angle steps.

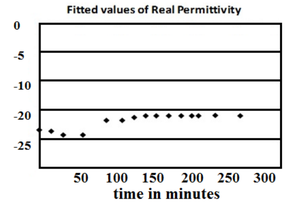

Fig. 5a Real permittivity

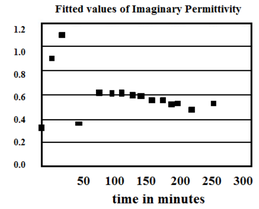

Fig. 5b Imaginary permittivity

RESULTS AND DISCUSSION

Monitoring Silver Layer Surface Permittivity Changes

Group 1B metals (silver / gold) have weak adhesion to glass. We deposited an adhesion promoting layer, chromium (group VIa) 2-3nm thick onto glass, forming covalent oxide surface bonds with hydroxyl groups. A 45nm silver film (±2nm) was sputtered, chosen from previous work, as deposition rate / optimal thickness are known. SPR curves were taken with air, water, or saline for data *vs.* theory. Cells show good temporal stability, as with previous liquid crystal cells **[13]**. A Vernier Salinity Standard NaCl Solution was added by syringe (0.8 ml) and sealed, halting cell evaporation. Reflectivity was recorded from a simulated marine environment, shown for a silver film, **fig. 3**, for 2 months of data, with a downward angle trend in SPR resonant reflectivity minima after 1389 hours of synthetic saline solution exposure.

RESULTS AND DISCUSSION

Fitting Experimental Data The technique minimises differences between data and theory, varying 3 parameters to achieve an optimal theory curve matching experimental data. Parameters iterative to minimise mean square error where:

$$\overline{\sigma^2} = \sum (R_i^t - R_i^e)^2$$

$R^t{}_i$ is the theoretical reflectivity at the *ith* measurement angle and $R^e{}_i$ is the experimental reflectivity at the same angle. Iterative steps are chosen by a method of swiftest descent. Partial derivative were calculated w.r.t. each of the parameters and the next search point in a direction opposed to the vector of the 3 derivatives where:

$$\begin{pmatrix} \epsilon' \\ \epsilon'' \\ t_l \end{pmatrix}_{i+1} = \begin{pmatrix} \epsilon' \\ \epsilon'' \\ t_l \end{pmatrix}_i - s \begin{pmatrix} \frac{\delta\overline{\sigma^2}}{\delta\epsilon'} \\ \frac{\delta\overline{\sigma^2}}{\delta\epsilon''} \\ \frac{\delta\overline{\sigma^2}}{\delta t_l} \end{pmatrix}$$

i is the *ith* parameters' estimate, *s* the step length to the next estimate, to achieve the least mean square error at the next point. Silver data vs minimised theoretical reflectivity is shown, **fig. 4** for a cell with permittivity: -18.47 + i0.33, for a 0.9nm AgO layer, similar to other workers [**14**]. After an initial bulk 'free-fit' to fresh cell data we allowed a 0.9nm layer to 'free-fit' real / imaginary permittivity until the routine found a minimum. De Rooij showed linear oxide thickness increased over time from 0.9nm; his data agrees with observed angle shifts. Fits were obtained 0 – 267 minutes after filling, with permittivity 'settling down' over time (**fig. 5a**, **fig. 5b**) displaying the complex unstable nature of 'corroded' metal. Some SPR workers explain surface permittivity temporal variations due to solvent molecules entering a metal [**15**] resulting in composite metal / electrolyte film with different permittivity. Multiple oxide layers may grow into films, or water penetrate metal through voids, altering properties. Silver oxidation is limited to water / air diffusion, but as this is not a flow, cell, no stirring occurs. Agitation *may* improve mass transfer to silver electrodes but likely disrupts polarisation. As we wanted to quantify static tank surface changes rather than flow pipes this was regarded unnecessary. Data acquisition was extensive, we obtained 35k cell data points, besides references.

CONCLUSIONS

1. **SPR angle minima plotted over time, shows linear correlation**
2. **Linear SPR coupling minima shift agrees with AgO growth**

Day 1 results indicated surface filling changes, as films were still intact after 6 months. 40% reflectivity change was observed between day 1 and 2, with 1 degree shift in minima. The SPR method quantifies values for surface permittivities in a synthetic marine environment, and may provide optical non-destructive evaluation of oxide growth rate for more reactive metals.

REFERENCES

1. Himour, A., Abderrahmane, S., Beliardouh, N.E., Zahzouh, M., Ghers, M., *Japanese Journal of Applied Physics*, 44(1), pp.305-10, (2005).
2. Tompkins, H., *Handbook of Ellipsometry,* ISBN-13: 978-0815514992, William Andrew, (2005).
3. Salah, N.H., *Surface Plasmon Resonance Sensing and Characterisation of Nano-Colloids for Nanotoxicology Applications*, PhD, Plymouth University, (2015).
4. Lavers, C.R., *Optical SPR Sensor for Corrosion Patent Applications*, British Patent Application No. 1611929.9, (2016).
5. Raising Awareness about Corrosion and Corrosion Protection around the World, *http://corrosion.org/* (accessed 31-10-2019).
6. Otto, A*., Z Phys* 216, pp. 398-410, (1968).
7. Kretschmann, E., and Raether, M., *Z.Naturf.,* 23(A), pp. 2135-36, 1968.
8. Lavers, C.R., *Thin Solid Films*, 230, 217-224, (1993).
9. Lavers, C.R., Jenkins, D., Cree, A., Salah, N., Findlay, M., *Proceedings of Sensors and Their Applications 18*, QMUL London, (2016).
10. Maxwell-Garnett, J.C., *Phil Trans* A203, 385, (1904).
[11. Ko, D.Y.K., and Sambles, J.R., *J. Opt., Am.,* 5, p. 1863, (1988).
12. Adachi, S., *The Handbook on optical constants of metals*, ISBN: 978-981-4405-94-2 World Scientific, (2012).
13. Innes, R.A., and Sambles, J.R., *Optics Commun.,* 64, 288, (1987).
[14. Rooij, A. de, *ESA Journal,* Vol. 13, pp.363-382. 1989.
15. Pollard, J.D., Sambles, J.R., and Bradberry, G.W., *J. Mod. Optics*, Vol. 37, pp. 841-846, (1990).